Icarus 232 (2014) 81–87

Contents lists available at ScienceDirect

Icarus

journal homepage: www.elsevier.com/locate/icarus

Origin of the peculiar eccentricity distribution of the inner cold Kuiper belt

A. Morbidelli [a,*], H.S. Gaspar [b,c], D. Nesvorny [d]

[a] Laboratoire Lagrange, UMR7293, Université de Nice Sophia-Antipolis, CNRS, Observatoire de la Côte d'Azur, Boulevard de l'Observatoire, 06304 Nice Cedex 4, France
[b] UNESP Univ. Estadual Paulista, FEG, GDOP, Av. Dr. Ariberto Pereira da Cunha, 333, CEP 12 516-410, Guaratinguetá, SP, Brazil
[c] Capes Foundation, Ministry of Education of Brazil, Caixa Postal 250, Brasília DF 70040-020, Brazil
[d] Southwest Research Institute, Boulder, CO 80302, United States

ARTICLE INFO

Article history:
Received 23 July 2013
Revised 20 December 2013
Accepted 29 December 2013
Available online 15 January 2014

Keywords:
Kuiper belt
Planetary dynamics
Resonances, orbital
Origin, Solar System

ABSTRACT

Dawson and Murray-Clay (Dawson and Murray-Clay [2012]. Astrophys. J., 750, 43) pointed out that the inner part of the cold population in the Kuiper belt (that with semi major axis $a < 43.5$ AU) has orbital eccentricities significantly smaller than the limit imposed by stability constraints. Here, we confirm their result by looking at the orbital distribution and stability properties in proper element space. We show that the observed distribution could have been produced by the slow sweeping of the 4/7 mean motion resonance with Neptune that accompanied the end of Neptune's migration process. The orbital distribution of the hot Kuiper belt is not significantly affected in this process, for the reasons discussed in the main text. Therefore, the peculiar eccentricity distribution of the inner cold population cannot be unequivocally interpreted as evidence that the cold population formed in situ and was only moderately excited in eccentricity; it can simply be the signature of Neptune's radial motion, starting from a moderately eccentric orbit. We discuss how this agrees with a scenario of giant planet evolution following a dynamical instability and, possibly, with the radial transport of the cold population.

1. Introduction

The Kuiper belt has a complex orbital structure and can be divided in multiple sub-populations (see Gladman et al., 2008 for a review). Among them are the cold and the hot populations, which are defined as the collections of objects inwards of the 1/2 resonance with Neptune (~48 AU) with, respectively, inclinations smaller or larger than 4°. The cold and hot populations have also distinct physical properties (see Morbidelli and Brown, 2004 for a review).

There is a quite general consensus that the hot population formed originally closer to the Sun, was dynamically excited by the perturbations from the giant planets and finally was transported into the Kuiper belt (Gomes, 2003; Levison et al., 2008). However, there is no consensus on the origin of the cold population. Some models argue that it also was transported into the Kuiper belt from a region closer to the Sun (Levison and Morbidelli, 2003; Levison et al., 2008), while others argue that the cold population formed locally (e.g. Parker et al., 2011; Batygin et al., 2011).

An important point in this debate was made by Dawson and Murray-Clay (2012). First they observed that the usual partition of the cold and hot populations according to the 4° inclination boundary is simplistic; in reality these populations have distinct, but partially overlapping inclination distributions (see Brown, 2001). Thus, to limit the contamination of the cold population by the hot population, they restricted their analysis to objects with inclination $i < 2°$, where the relative fraction of low-inclination "hot" objects is expected to be negligible. Then they showed that, inside of 43.5 AU, this low-inclination population has also small eccentricities ($e \lesssim 0.05$), even though orbits would be stable up to $e \sim 0.1$ (Lykawka and Mukai, 2005a). The hot population, in fact, has eccentricities up to this limit. The lack of moderate eccentricity orbits in the cold population obviously cannot be explained by observational biases. Dawson and Murray-Clay therefore interpreted this result as evidence that the cold Kuiper belt was only very moderately excited relative to its original quasi-circular and coplanar orbits. This argues against models in which the cold population originates closer to the Sun and is implanted into the Kuiper belt, because such models predict a cold population with an eccentricity distributions covering the whole stability range.

Given the importance of this argument, we have decided to revisit the problem of the eccentricity distribution of the cold Kuiper belt. In Section 2 we redo the same analysis as Dawson and Murray-Clay, but using proper elements instead of osculating elements. Our results confirm theirs, but we notice that the transition between the inner part of the cold population, where eccentricities

* Corresponding author. Fax: +33 4 92003118.
E-mail addresses: morby@oca.eu (A. Morbidelli), helton.unesp@gmail.com (H.S. Gaspar).

0019-1035/$ - see front matter © 2014 Elsevier Inc. All rights reserved.
http://dx.doi.org/10.1016/j.icarus.2013.12.023

are all small, to the outer part, where the eccentricities cover a wider range, happens exactly at the 4/7 mean motion resonance with Neptune. This suggests that this resonance might have played a role in sculpting the inner cold belt during a phase of outward migration. Then, in Section 3 we conduct migration experiments, testing different migration timescales and eccentricities of Neptune. Section 4 analyzes more in details how moderate-eccentricity cold Kuiper belt objects are removed by resonance sweeping and compares their evolution with that of high inclination bodies. Our conclusions are discussed in Section 5.

2. Distribution of proper elements and stability map for the cold Kuiper belt

We have selected all TNOs from the MPC catalog with semi major axis larger than 25 AU and orbits determined from observations covering at least three oppositions. Such procedure selected a set of 811 TNOs. For each of these objects we computed numerically the orbital proper elements using integrations covering 132 My. The proper semi major axis was computed by numerical average of the values recorded during the simulation, with an output time-step of 1000 y. For the proper eccentricities and inclinations, the computational procedure was more elaborated, although standard (Knežević and Milani, 2000). We first computed the Fourier series of $(h(t), k(t))$ and $(p(t), q(t))$, where:

$$\begin{aligned} h(t) &= e(t)\cos[\varpi(t)] \\ k(t)) &= e(t)\sin[\varpi(t)] \\ p(t) &= i(t)\cos[\Omega(t)] \\ q(t)) &= i(t)\sin[\Omega(t)] \end{aligned} \quad (1)$$

and $e(t), i(t), \varpi(t)$ and $\Omega(t)$ are the values of eccentricity, inclination, longitude of perihelion and longitude of node recorded over time t. We then removed from the series expansions the terms with frequencies close (i.e. within one arcsec/y) to the proper frequencies of the planets. Finally, we selected as proper eccentricity and inclination the coefficients of the largest remaining term in the each of the two Fourier series.

In order to evaluate the accuracy of proper eccentricity and inclination, we performed the procedure described above for the first and the second halves of the whole integration, i.e., 65.536 My. Then, we adopted as an estimate of the error, the largest difference among the proper elements calculated for the whole integration time-span and those computed in each of the two half time-spans. The relative accuracy in proper semi major axis was always better than 3×10^{-4}. The absolute accuracies in proper eccentricity and inclinations were better than 0.01° and 0.1° throughout the region of interest (i.e. inside of 44 AU and not in the 4/7 mean motion resonance with Neptune).

Once in possession of this proper element catalog, following Dawson and Murray-Clay we retained as members of an "uncontaminated cold population" the objects with proper inclination smaller than 2°. Fig. 1 shows the distribution of the selected objects (dots) in proper semi major axis vs. eccentricity plane.

We also computed a new stability map. In fact, the map used by Dawson and Murray-Clay, from Lykawka and Mukai (2005a), was computed for a wide range of inclinations, whereas here we are interested to very low inclinations only. We could have used the stability map in Duncan et al. (1995), which was computed for $i = 1°$, but the latter was quite sparse, due to the computing limitations of the time. Moreover, both Lykawka and Mukai and Duncan et al. reported their maps relative to the initial osculating elements. Here, for a consistent comparison with the proper elements of the real objects, we needed a map computed in proper elements space.

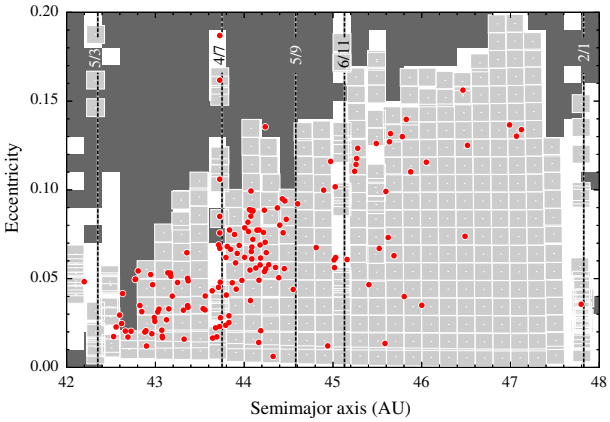

Fig. 1. The dots show the distribution of proper semi major axis and proper eccentricities of the Kuiper belt objects with well-defined orbits and proper inclination smaller than 2°. The light-gray squares denote the regions of proper element space that are stable in 4 Gy simulations and the dark-gray squares denote the initial orbital elements of unstable particles. White color is the background. The light-gray squares are not regularly spaced because the application mapping the initial conditions (regularly spaced) to proper elements is not linear. The vertical dashed lines depict the main mean motion resonances as labeled.

To compute the stability map, we proceeded as follows. We adopted a grid of particles' initial conditions, with osculating elements in the following ranges: 42 AU < a < 48 AU, $0 < e < 0.2$ and $0 < i < 2°$, with resolutions of 0.2 AU in a, 0.01 in e and 0.5° in i. The secular angles Ω and ϖ were set equal to 0°. Each particle was integrated for 132 My. We then computed their proper elements following the same procedure described above. Finally, we continued the simulations for 4 Gy in order to asses the long-term survival of the test particles.

To construct Fig. 1, for each given pair of initial a and e, we selected the particle with the smallest value of proper inclination. Then, for the particles that survived in the 4 Gy integration (i.e. they did not encounter Neptune within a Hill radius within this time), we plotted on a white background a light-gray square of size 0.2 AU × 0.01 centered on their values of proper semi major axis and eccentricity measured on the first 132 My. Moreover, particles that did not survive were denoted by dark-gray squares centered on the initial pair of osculating semi major axis and eccentricity.

The stability map of Fig. 1 shows few surprises. In general, particles are unstable at large eccentricity and stable at low eccentricity, where the perihelion distance is larger than ~38–40 AU. Mean motion resonances represent the exception to this general rule. The light-gray squares at large eccentricity are all associated to mean motion resonances, as well as the vertical white columns at low or moderate eccentricities. Some mean motion resonances, therefore, clearly stand out from the stability map, and they are labeled on the figure.

In general, as expected, the dots fall on light-gray squares. Those that do not, are associated to mean motion resonances. In fact, in a mean motion resonance there is a third dimension characterizing the orbit: the resonant amplitude. It is well possible that none of the test particles that we used for the stability map sampled the orbit of a real particle because their libration amplitude is different. In this case, a dot is plotted over the white background.

Overall, Fig. 1 confirms the results of Dawson and Murray-Clay. Inside of 43.5 AU, all real objects have small eccentricities, barely exceeding 0.05. The stability map, however, ranges up to 0.1 in the 42.2–42.6 AU region. Thus, there is clearly a stable region (approximately in the range $0.05 < e < 0.1$) in the inner belt that is not inhabited by the cold population. At a closer inspection,